PCP
PLANT & CELL PHYSIOLOGY

Reactive Carbonyl Species Mediate ABA Signaling in Guard Cells

Md. Moshiul Islam[1,2,5], Wenxiu Ye[1,5], Daiki Matsushima[1], Shintaro Munemasa[1], Eiji Okuma[1], Yoshimasa Nakamura[1], Md. Sanaullah Biswas[3], Jun'ichi Mano[3,4] and Yoshiyuki Murata[1,*]

[1]Graduate School of Environmental and Life Science, Okayama University, 1-1-1 Tsushima-Naka, Okayama, 700-8530 Japan
[2]Department of Agronomy, Bangabandhu Sheikh Mujibur Rahman Agricultural University, Gazipur 1706, Bangladesh
[3]Graduate School of Agriculture, Yamaguchi University, Yoshida 1677-1, Yamaguchi, 753-8515 Japan
[4]Science Research Center, Yamaguchi University, Yoshida 1677-1, Yamaguchi, 753-8515 Japan
[5]These authors contributed equally to this work
*Corresponding author: E-mail, muta@cc.okayama-u.ac.jp; Fax, +81-86-251-8388.
(Received November 24, 2015; Accepted September 16, 2016)

Regular Paper

Drought is responsible for a massive reduction in crop yields. In response to drought, plants synthesize the hormone ABA, which induces stomatal closure, thus reducing water loss. In guard cells, ABA triggers production of reactive oxygen species (ROS), which is mediated by NAD(P)H oxidases. The production of ROS is a key factor for ABA-induced stomatal closure, but it remains to be clarified how the production of ROS is transduced into downstream signaling components in guard cells. We investigated roles of reactive carbonyl species (RCS) in ABA-induced stomatal closure using transgenic tobacco (*Nicotiana tabacum*) overexpressing Arabidopsis 2-alkenal reductase (AER-OE), which scavenges RCS. ABA and hydrogen peroxide (H_2O_2) induced accumulation of RCS including acrolein and 4-hydroxy-(*E*)-2-nonenal in wild-type tobacco but not in AER-OE. Stomatal closure and RCS accumulation in response to ABA and H_2O_2 were inhibited in AER-OE unlike in the wild type, while ABA-induced H_2O_2 production in guard cells was observed in AER-OE as well as in the wild type. Moreover, ABA inhibited inward-rectifying K^+ channels in wild-type guard cells but not in AER-OE guard cells. These results suggest that RCS is involved in ABA-induced stomatal closure and functions downstream of H_2O_2 production in the ABA signaling pathway in guard cells.

Keywords: ABA • Reactive carbonyl species • Reactive oxygen species • Stomatal closure.

Abbreviations: AER, alkenal reductase; DNP, dinitrophenylhydrazone; DNPH, 2,4-dinitrophenylhydrazine; DPI, diphenylene iodonium chloride; FDA, fluorescein diacetate; GCP, guard cell protoplast; GSH, glutathione; H_2DCF-DA, 2',7'-dichlorodihydrofluorescein diacetate; HHE, 4-hydroxy-(*E*)-2-hexenal; HNE, 4-hydroxy-(*E*)-2-nonenal; K_{in}^+ channels; inward-rectifying K^+ channels, RCS, reactive carbonyl species; ROS, reactive oxygen species; WT, wild type.

Introduction

Stomata, formed by pairs of guard cells, play a critical role in regulation of CO_2 uptake and transpirational water loss, and protection from invasion by microorganisms (Schroeder et al. 2001, Melotto et al. 2008). Guard cells respond to a variety of abiotic and biotic stresses (Shimazaki et al. 2007, Murata et al. 2015, Ye et al. 2015). ABA induces stomatal closure to suppress water loss in plants subjected to drought stress (Assmann and Shimazaki 1999, Schroeder et al. 2001). Hence, disruption of the ABA synthesis pathway or the ABA signaling pathway causes malfunction of stomatal movements, which threatens the survival of plants under drought stress (Nambara and Marion-Poll 2005, Cutler et al. 2010, Hubbard et al. 2010).

ABA-induced stomatal closure is accompanied by production of reactive oxygen species (ROS) in guard cells (Pei et al. 2000, Murata et al. 2001, Uraji et al. 2012). ABA-induced ROS production is mediated by the plasma membrane NAD(P)H oxidases AtrbohD and AtrbohF in *Arabidopsis thaliana* (Kwak et al. 2003). ABA-induced stomatal closure is also accompanied by depletion of glutathione (GSH) in Arabidopsis guard cells (Akter et al. 2012). Moreover, ABA and H_2O_2 suppress plasma membrane inward-rectifying K^+ channels (K_{in}^+ channels) in guard cells, which is favorable for stomatal closure (Zhang et al. 2001, Yin et al. 2013). However, although it is well known that ROS mediate ABA signaling in guard cells (Pei et al. 2000, Kwak et al. 2003), the mechanism by which the production of ROS is transduced into downstream signal components in guard cells remains to be clarified.

A variety of stresses induce production of ROS in plants, and the accumulating ROS oxidize lipids, especially polyunsaturated fatty acids. Oxidized lipids decompose spontaneously or are degraded by enzymes to form reactive compounds including aldehydes, ketones and hydroxyl acids (Mueller 2004, Mosblech et al. 2009, Mano 2012). Aldehydes and ketones containing α,β-unsaturated carbonyl structure are termed as reactive carbonyl species (RCS). Accumulated RCS impair growth of plants because RCS are toxic to plants (Mano 2012). Alkenal reductase (AER), aldehyde dehydrogenase (ALDH), aldo-keto reductase (AKR) and aldehyde reductase (ALR) detoxify RCS (Oberschall et al 2000, Mano et al. 2002, Stiti et al. 2011, Yamauchi et al. 2011) and the overexpression of AER, ALDH, AKR and ALR improves stress tolerance in plants (Oberschall

Plant Cell Physiol. 57(12): 2552–2563 (2016) doi:10.1093/pcp/pcw166, Advance Access publication on 12 November 2016, available online at www.pcp.oxfordjournals.org

et al. 2000, Mano et al. 2005, Papdi et al. 2008, Huang et al. 2008, Yin et al. 2010, Turóczy et al. 2011).

RCS function downstream of ROS in NF-κB-induced inflammatory response in animal cells (Yadav and Ramana 2013) and in aluminum-induced root injury response in tobacco plants (Yin et al. 2010). RCS deplete GSH through conjugation in the tobacco hypersensitive response (Davoine et al. 2006). Very recently, Biswas and Mano (2015) showed that RCS act as triggers in the H_2O_2-induced and NaCl-induced programmed cell death in plants. The action of RCS is accounted for by the activation of caspase-like proteases (Biswas and Mano 2016). These results clearly demonstrate that RCS, downstream products of ROS, play a role as signaling agents.

In this study, we tested whether or not RCS function downstream of ROS production in guard cell ABA signaling. We examined stomatal movements, production of H_2O_2 and RCS in guard cells, and plasma membrane K_{in}^+ channel activities in guard cells, and assessed transpirational water loss and drought tolerance using transgenic tobacco (*Nicotiana tabacum*) plants overexpressing *A. thaliana* AER in order to scavenge RCS. Both ABA and H_2O_2 induced RCS production and stomatal closure, and RCS induced stomatal closure, which is accompanied by inactivation of K_{in}^+ channels. Based on these results, we provide a new model of the ABA signaling pathway in guard cells.

Results

ABA-induced stomatal closure in AER-OE

To determine whether RCS mediate ABA-induced stomatal closure, we analyzed stomatal responses to ABA in transgenic tobacco (*N. tabacum*) plants overexpressing *A. thaliana* AER (At5g16970) (AER-OE plants; Mano et al. 2005). AER catalyzes the reduction of 2-alkenal to *n*-alkanal, to decrease the reactivity of the former by 10-fold (Mano et al. 2002). Application of 1 and 10 μM ABA to epidermal tissues of wild-type (WT) plant leaves induced stomatal closure ($P < 0.002$ at 1 μM, $P < 10^{-3}$ at 10 μM) (Fig. 1). ABA-induced stomatal closure was impaired in three AER-OE plants, P1#11 ($P = 0.10$ at 1 μM, $P = 0.07$ at 10 μM), P1#14 ($P = 0.13$ at 1 μM, $P = 0.08$ at 10 μM) and P1#18 ($P = 0.17$ at 1 μM, $P = 0.13$ at 10 μM) (Fig. 1). Impairment of the ABA-induced stomatal closure by AER suggests that RCS mediates the ABA signal for stomatal closure.

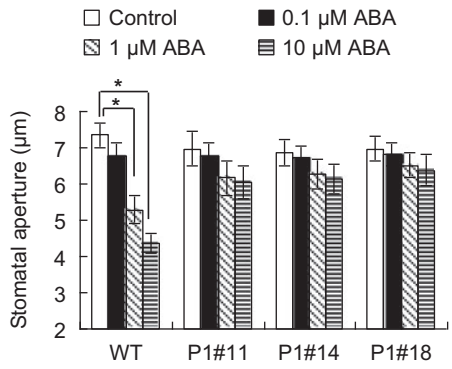

Fig. 1 ABA-induced stomatal closure in tobacco. ABA-induced stomatal closure in wild-type (WT) and AER-OE plants P1#11, P1#14 and P1#18. Excised leaves were treated with ABA for 2 h. Averages from three independent experiments (60 total stomata per bar) are shown. Error bars represent the SEM. An asterisk denotes a significant difference ($P < 0.05$).

AER activities

We measured AER activities in epidermal tissues of the WT and the AER-OE plant, P1#18. AER activities of P1#18 were higher than those of the WT not only when plants were untreated with ABA or H_2O_2 but also when treated with ABA and H_2O_2 (Fig. 2). These results suggest that RCS levels in AER-OE plants are lower than those in the WT.

ABA- and H_2O_2-induced production of RCS

To clarify that RCS are produced downstream of H_2O_2 production in guard cell ABA signaling, we quantified RCS production in epidermal tissues of tobacco leaves treated with ABA and H_2O_2 for 30 min using reverse-phase HPLC after derivatization with 2,4-dinitrophenylhydrazine (DNPH). Typical chromatograms for the epidermal tissues treated with ABA and H_2O_2 are shown in Fig. 3A. Treatment with either 50 μM ABA or 1 mM H_2O_2 significantly increased the contents of acrolein (Fig. 3A, B) and 4-hydroxy-(*E*)-2-nonenal (HNE) (Fig. 3A, C) in epidermal tissues of the WT. The increase in acrolein in response to both ABA and H_2O_2 was 1 mol g FW^{-1} and that of HNE was 4 nmol g FW^{-1}. ABA and H_2O_2 also significantly increased the contents of 4-hydroxy-(*E*)-2-hexenal (HHE), (*E*)-2-pentenal, (*E*)-2-heptenal, (*Z*)-3-hexenal, formaldehyde, acetaldehyde, propionaldehyde, *n*-hexanal, *n*-heptanal and acetone in epidermal tissues of the WT (Figs. 3A, 4). These results indicate that ABA and H_2O_2 induce RCS production in epidermal tissues of leaves. The increment in concentrations of acrolein and HNE in epidermal tissues treated with ABA and H_2O_2 are evaluated at approximately 1 and 4 μM, respectively, assuming that 1 g of fresh weight is equivalent to 1 ml. These values are average concentrations in

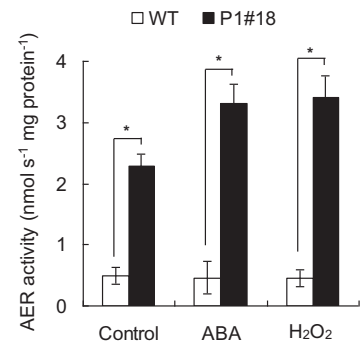

Fig. 2 AER activities in leaves of the wild-type (WT) and the AER-OE plant P1#18. Epidermal tissues of the WT and P1#18 were treated with ABA and H_2O_2. Proteins were extracted from epidermal tissues and AER activity in the extract was determined as described in the Materials and Methods. Averages from three independent experiments are shown. Error bars represent the SEM. An asterisk denotes a significant difference ($P < 0.05$).

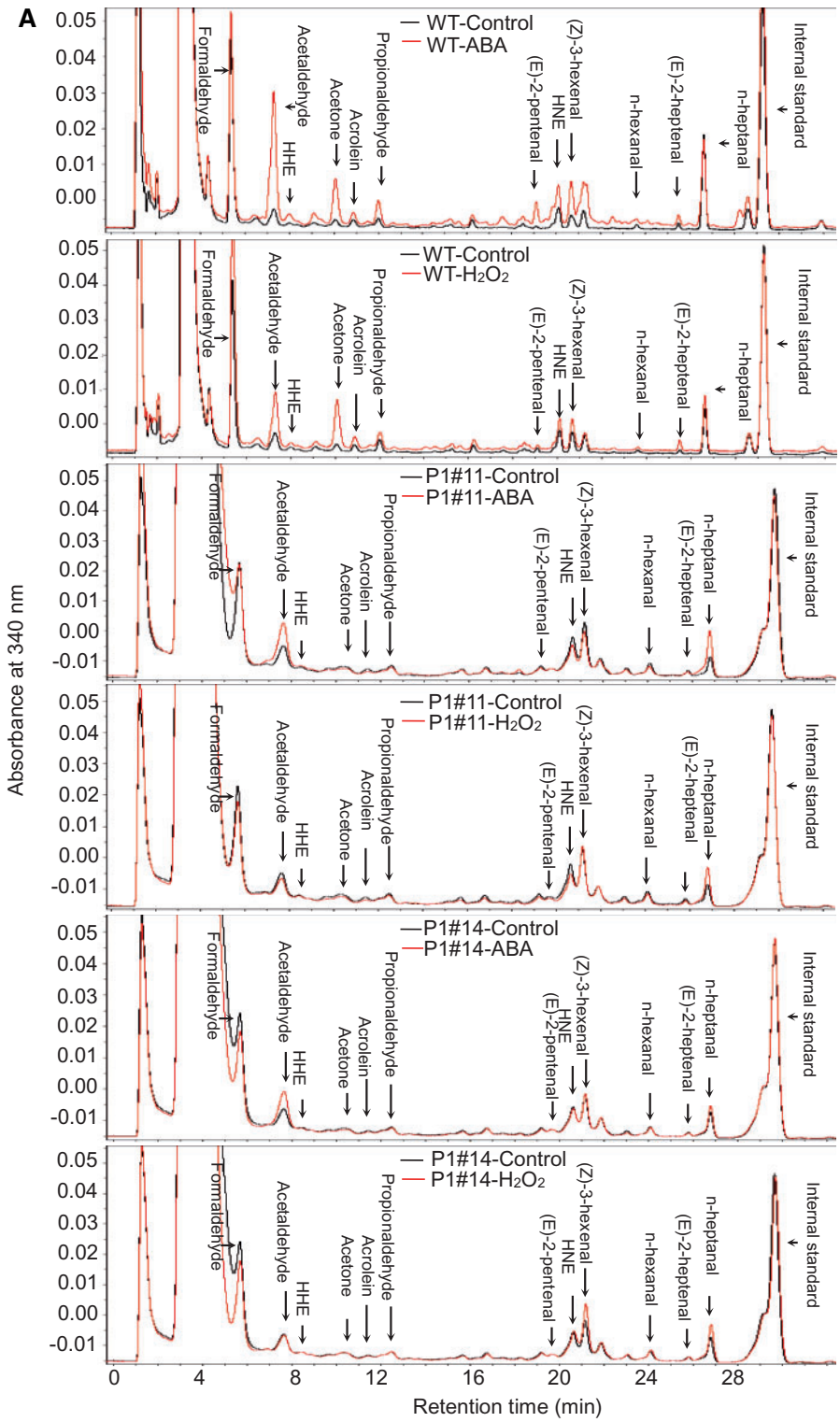

Fig. 3 Typical chromatograms for the epidermal tissues treated with or without ABA and H_2O_2 for 30 min. (A) Typical chromatograms of the DNP derivatives of reactive carbonyl species extracted from control (black lines) and ABA- and H_2O_2-treated (red lines) epidermal tissues of wild-type (WT) and AER-OE plants P1#11, P1#14 and P1#18. Identified reactive carbonyl species are labeled at the top of each peak. DNP derivatives of reactive carbonyl species were detected at 340 nm. (B) Contents of acrolein in the epidermal tissues of the WT, P1#11, P1#14 and P1#18. (C) Contents of HNE in the epidermal tissues of the WT, P1#11, P1#14 and P1#18. Error bars represent the SEM (n = 5). An asterisk denotes a significant difference ($P < 0.05$).

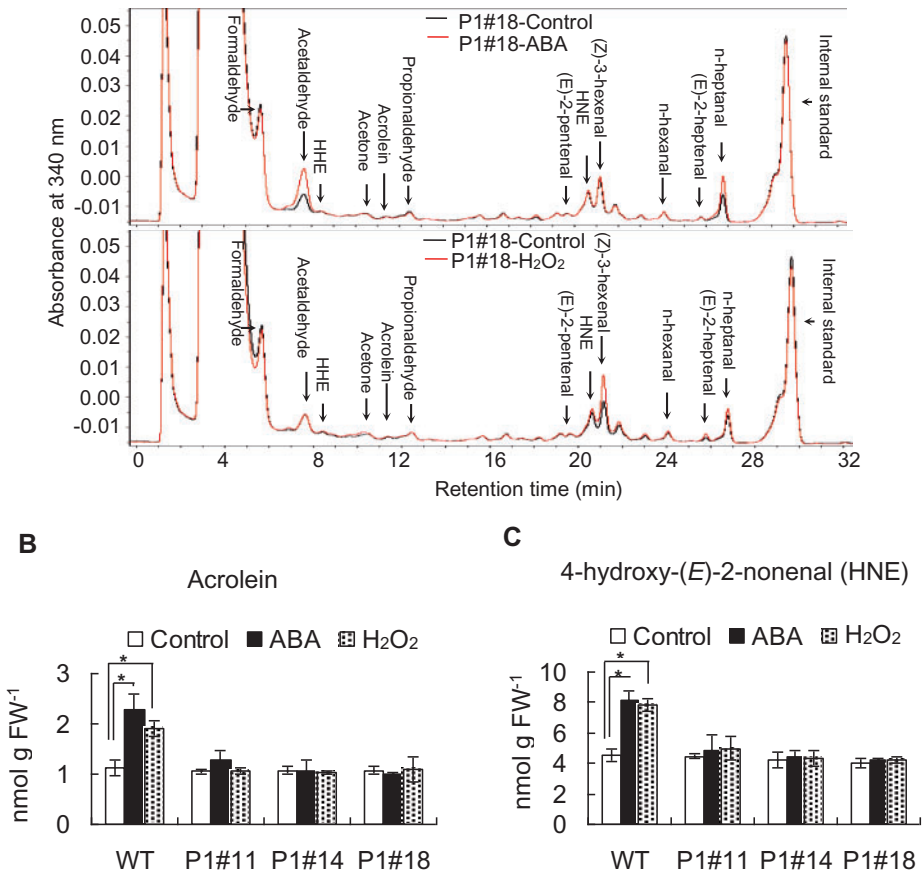

Fig. 3 Continued.

the epidermal tissues. The actual increase in the levels of these aldehydes in guard cells should be >10 μM because ABA induces detectable ROS production only in guard cells but not in other epidermal cells and because guard cells occupy <10% (v/v) of the epidermal tissue used in this experiment.

We measured RCS contents in epidermal tissues from AER-OE leaves. Neither ABA nor H_2O_2 significantly increased contents of most species of RCS, such as acrolein and HNE, in epidermal tissues from AER-OE leaves (P1#11, P1#14 and P1#18) (**Figs. 3, 4**). These results support that RCS mediates ABA-induced stomatal closure.

We also determined RCS contents in epidermal tissues of the WT and the AER-OE plant, P1#18 treated with ABA for 5–120 min (**Supplementary Figs. S1, S2**). The contents of RCS in epidermal tissues of the WT were elevated by ABA treatment within 30 min and were kept substantially constant from 30 to 120 min (**Supplementary Figs. S1, S2**). In contrast to the RCS levels in the WT, the RCS levels in P1#18 were not drastically changed in response to ABA (**Supplementary Figs. S1, S2**).

RCS-induced stomatal closure in AER-OE plants

To clarify that RCS mediates ABA-induced stomatal closure, we tested whether acrolein and HNE induce stomatal closure. Application of acrolein at 10 and 100 μM induced stomatal closure in the WT ($P < 0.02$ for 10 μM acrolein, $P < 0.0008$ for 100 μM acrolein), and HNE at 10 and 100 μM also induced stomatal closure in the WT ($P < 0.01$ for 10 μM HNE, $P < 0.001$ for 100 μM HNE) (**Fig. 5A, B**). Moreover, the acrolein- and the HNE-induced stomatal closure was inhibited in AER-OE plants, P1#11 ($P = 0.07$ for 10 μM acrolein, $P < 0.02$ for 100 μM acrolein, $P = 0.14$ for 10 μM HNE, $P < 0.03$ for 100 μM HNE), P1#14 ($P = 0.08$ for 10 μM acrolein, $P < 0.01$ for 100 μM acrolein, $P = 0.16$ for 10 μM HNE, $P < 0.03$ for 100 μM HNE) and P1#18 ($P = 0.1$ for 10 μM acrolein, $P < 0.03$ for 100 μM acrolein, $P = 0.15$ for 10 μM HNE, $P < 0.04$ for 100 μM HNE) (**Fig. 5A, B**). These results also suggest that ABA induces stomatal closure via RCS production.

Reversibility of RCS-induced stomatal closure

Because RCS at higher concentrations are toxic, there is a possibility that acrolein and HNE damaged guard cells irreversibly and caused stomatal closure. If the stomatal closure by these RCS is a physiological response that is observed upon ABA application, the stomatal response has to be reversible. Treatment with 100 μM acrolein and 100 μM HNE for 2 and 4 h induced stomatal closure, and stomatal apertures at 4 h were slightly narrower than those at 2 h (**Fig. 5C, D;** filled square). When the bathing solution supplemented with acrolein or HNE was replaced with the bathing solution without acrolein or HNE, stomata significantly reopened in 2 h ($P <$

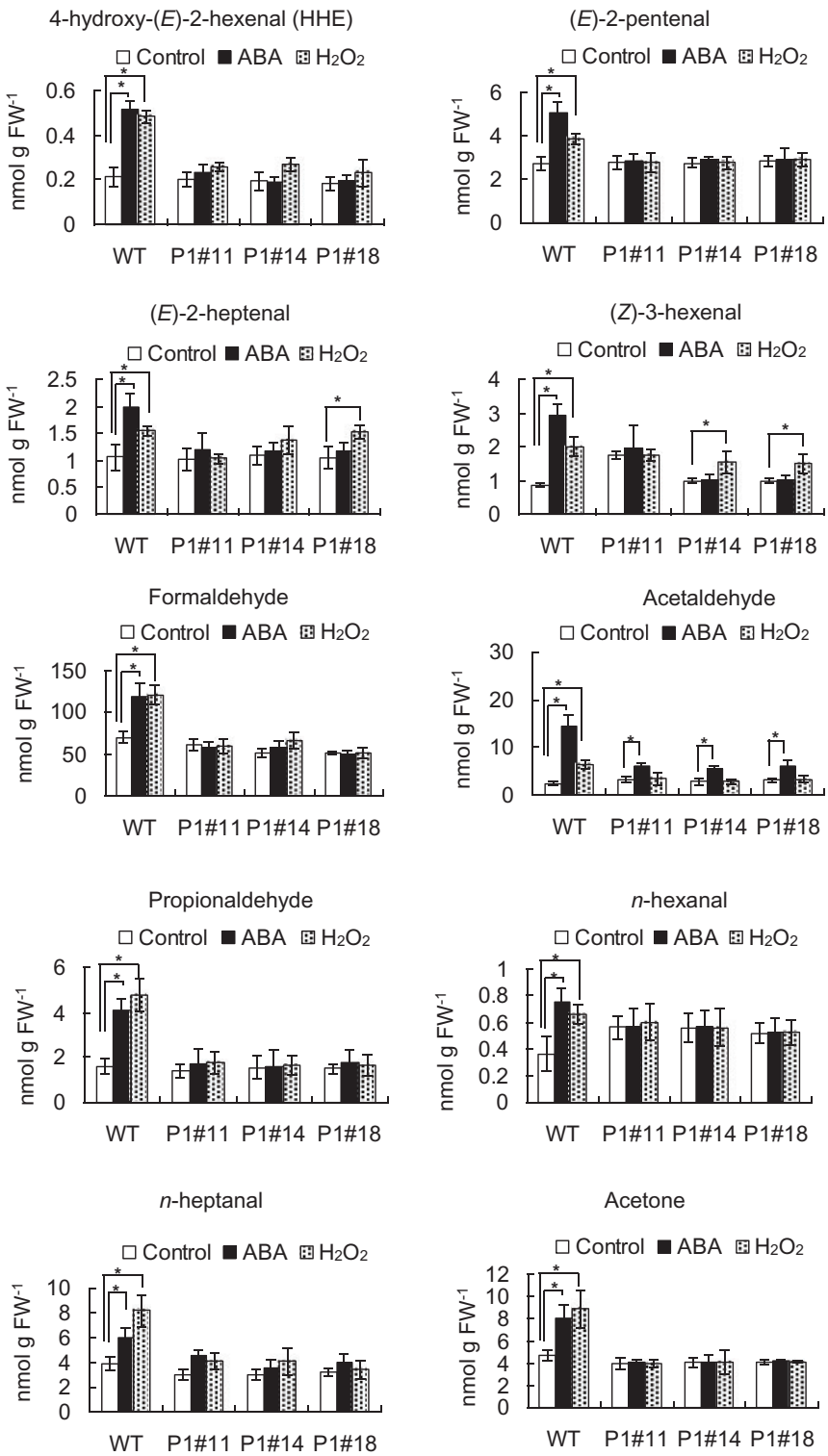

Fig. 4 Content of reactive carbonyl species in the epidermal tissues of wild-type (WT) and AER-OE plants P1#11, P1#14 and P1#18 treated with or without ABA and H_2O_2 for 30 min. Excised leaves of 5- to 7-week-old plants were blended for 25 s and epidermal tissues were collected and floated on an assay solution containing 5 mM KCl, 50 μM $CaCl_2$ and 10 mM MES-Tris, pH 6.15, for 2 h in the light followed by the addition of ABA or H_2O_2. Error bars represent the SEM (n = 5). An asterisk denotes a significant difference ($P < 0.05$).

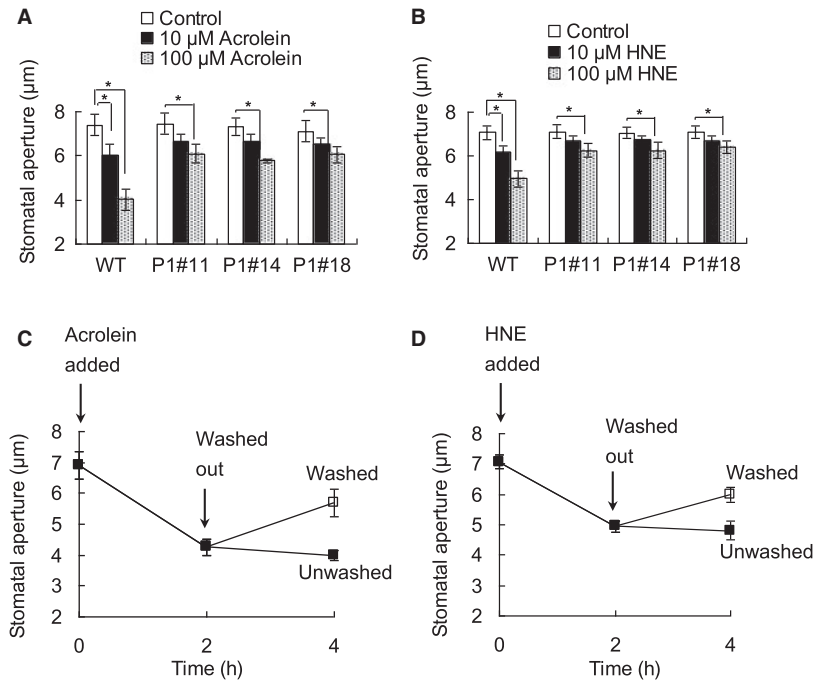

Fig. 5 Stomatal movement in response to acrolein and HNE. (A) Acrolein-induced stomatal closure in wild-type (WT) and AER-OE plants P1#11, P1#14 and P1#18. Excised leaves were treated with acrolein for 2 h. (B) HNE-induced stomatal closure in the WT, P1#11, P1#14 and P1#18. Excised leaves were treated with HNE for 2 h. (C) Stomatal movement in WT tobacco in the presence (filled square) or absence (open square) of 100 μM acrolein for 2 h after 2 h pre-treatment with 100 μM acrolein. (D) Stomatal movement in the WT in the presence (filled square) or absence (open square) of 100 μM HNE for 2 h after 2 h pre-treatment with 100 μM HNE. Averages from three independent experiments are shown. Error bars represent the SEM. An asterisk denotes a significant difference ($P < 0.05$).

0.008 for acrolein, $P < 0.004$ for HNE) (**Fig. 5C, D;** open square). Thus acrolein and HNE induce reversible stomatal closure, suggesting that RCS functions physiologically as a second messenger in the ABA signaling pathway in guard cells.

Guard cell viability

We assessed the viability of WT guard cells using fluorescein diacetate (FDA). Guard cells treated with acrolein or HNE at 100 μM for 2 h were stained with FDA for 5 min (**Supplementary Fig. S3**). When untreated with acrolein or HNE (control), 57.7% guard cells showed green fluorescence and when treated with acrolein and HNE treatment, 50.9% ($P = 0.18$) and 49.5% ($P = 0.13$) guard cells emitted fluorescence (**Supplementary Fig. S3**). These results indicate that acrolein and HNE at up to 100 μM do not significantly affect the viability of guard cells. These results suggest that RCS including acrolein and HNE at up to 100 μM function as signaling mediators without cytotoxicity.

ABA-induced H_2O_2 production in AER-OE guard cells

We examined ABA-induced H_2O_2 production in tobacco AER-OE guard cells using an H_2O_2-sensitive fluorescence dye, 2′,7′-dichlorodihydrofluorescein diacetate (H_2DCF-DA). Application of 50 μM ABA induced H_2O_2 production in guard cells of WT ($P < 0.001$) and the three AER-OE plants, P1#11 ($P < 0.003$), P1#14 ($P < 10^{-3}$) and P1#18 ($P < 0.001$) (**Fig. 6A**), indicating that scavenging RCS by AER did not affect ABA-induced H_2O_2 production. Moreover, ABA- and H_2O_2-induced stomatal closure was inhibited in the AER-OE plants (**Figs. 1, 6B**) and H_2O_2 induced RCS production (**Figs. 3, 4**). Taken together, these results suggest that RCS is generated downstream of ROS production in the guard cell ABA signaling pathway.

To confirm that the RCS generation in guard cells depends on the ROS production, we evaluated the effect of the NAD(P)H oxidase inhibitor diphenylene iodonium chloride (DPI) on ABA-induced RCS accumulation. Application of 25 and 50 μM DPI inhibited ABA-induced RCS accumulation in the WT (**Fig. 7A**) but not stomatal closure induced by 100 μM acrolein (**Fig. 7B**). These results also suggest that RCS is generated downstream of ROS production in the guard cell ABA signaling pathway.

Suppression of K_{in}^+ channel currents by ABA and acrolein in guard cells

ABA suppresses K_{in}^+ channel currents in the guard cell plasma membrane, which is favorable for stomatal closure (Saito et al. 2008, Uraji et al. 2012, Yin et al. 2013). Pre-treatment with 10 μM ABA suppressed K_{in}^+ channel currents in WT guard cell protoplasts (GCPs; $P < 0.001$ at −180 mV) (**Fig. 8A, B**) but not in GCPs of the AER-OE plant P1#18 ($P = 0.15$ at −180 mV) (**Fig. 8C, D**). Application of 10 μM acrolein also suppressed K_{in}^+ channel currents in WT GCPs ($P < 0.05$ at −180 mV) (**Fig. 8E, F**) but not in P1#18 GCPs ($P = 0.15$ at −180 mV) (**Fig. 8G, H**). Furthermore, H_2O_2 significantly inhibited K_{in}^+ channel currents in WT GCPs ($P < 0.05$ at −180 mV) (**Supplementary Fig. S4**) but not in P1#18 GCPs ($P = 0.97$ at −180 mV) (**Supplementary Fig. S4**). These results suggest that

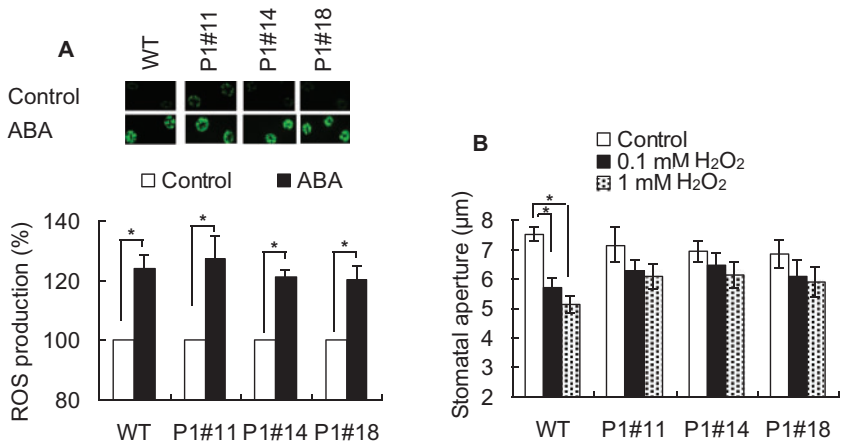

Fig. 6 ABA-induced H_2O_2 production in guard cells of the wild type (WT) and AER-OE P1#11, P1#14 and P1#18. (A) Effects of 50 μM ABA on H_2O_2 production in guard cells of the WT, P1#11, P1#14 and P1#18. The vertical scale represents the percentage of H_2DCF-DA fluorescence when the fluorescent intensities obtained from ABA-treated cells are normalized to the control value taken as 100% (white bars). Note that the control values for guard cells of P1#11 (7.28 ± 0.44), P1#14 (7.09 ± 0.57) and P1#18 (6.80 ± 0.62) were not significantly different from that of WT guard cells (6.99 ± 0.47). Bars indicate averages of three independent experiments (at least 60 guard cells). (B) H_2O_2-induced stomatal closure in the WT, P1#11, P1#14 and P1#18. Averages from three independent experiments (60 total stomata per bar) are shown. Error bars represent the SEM. An asterisk denotes a significant difference ($P < 0.05$).

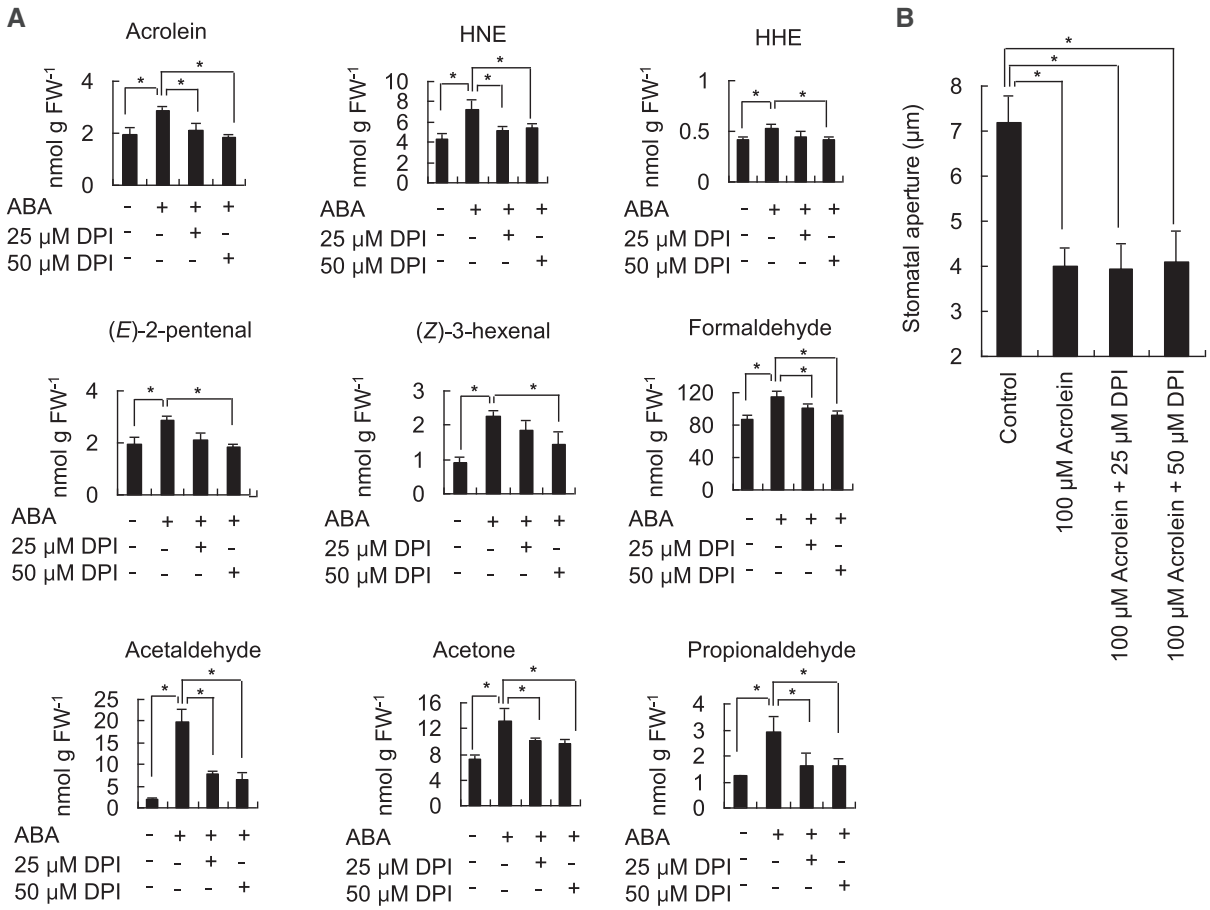

Fig. 7 Effects of the NAD(P)H oxidase inhibitor diphenylene iodonium chloride (DPI) on ABA-induced RCS accumulation and acrolein-induced stomatal closure. (A) Effect of DPI on ABA-induced RCS accumulation in the epidermal tissues of wild-type (WT) tobacco. Excised leaves of 5- to 7-week-old plants were blended for 25 s and epidermal tissues were collected and floated on an assay solution containing 5 mM KCl, 50 μM $CaCl_2$ and 10 mM MES-Tris, pH 6.15, for 2 h in the light followed by the addition of ABA. Averages from three independent experiments are shown. (B) Effect of DPI on stomatal closure induced by 100 μM acrolein in the epidermal tissues of WT tobacco. Excised leaves were treated with acrolein for 2 h. Averages from three independent experiments (60 total stomata per bar) are shown. Error bars represent the SEM. An asterisk denotes a significant difference ($P < 0.05$).

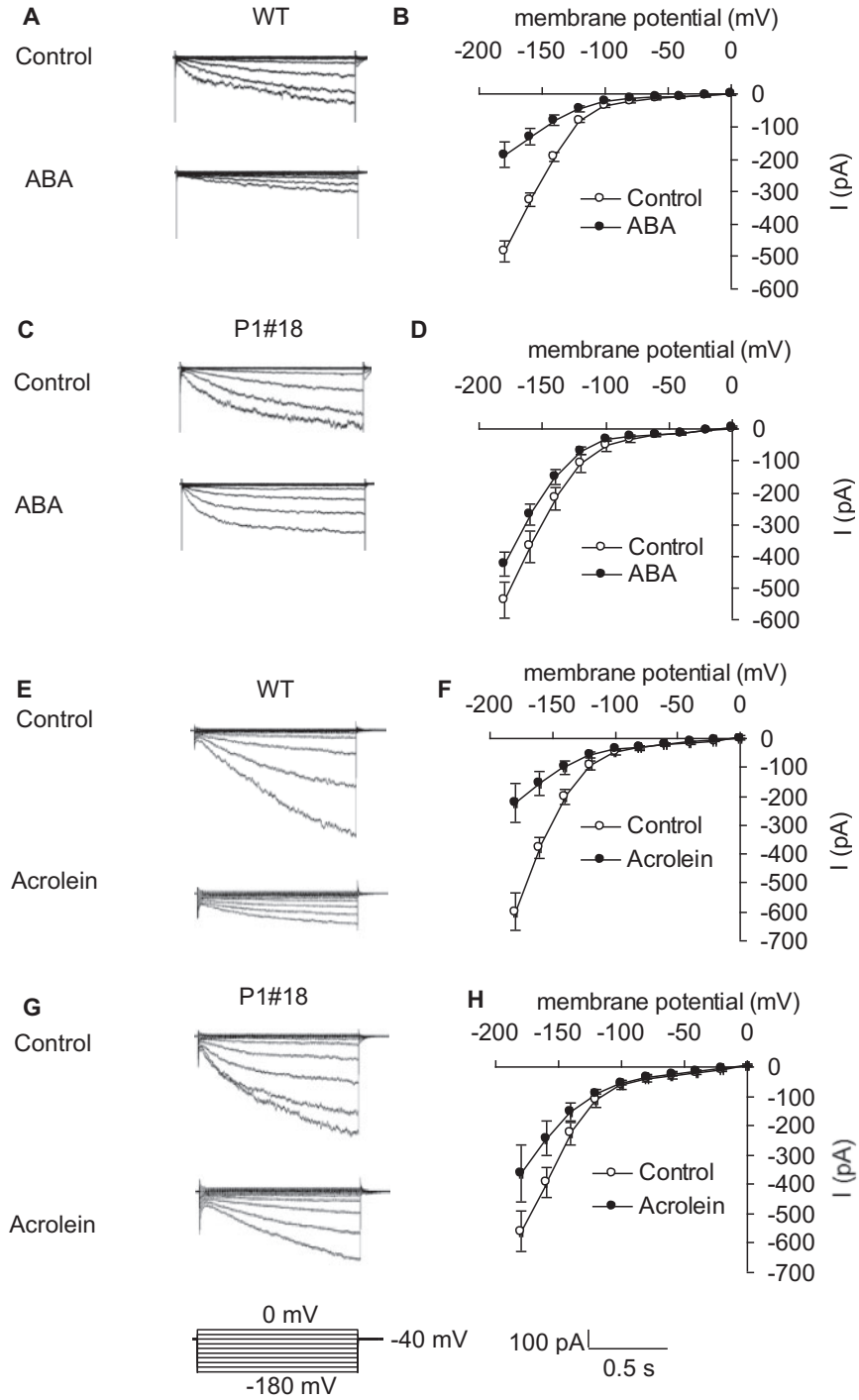

Fig. 8 ABA and acrolein inhibition of K_{in}^+ channel currents in GCPs of the wild-type (WT) and AER-OE P1#18. (A) K_{in}^+ channel currents in the WT treated without (top trace) or with 10 μM ABA (bottom trace). (B) Steady-state current–voltage relationship for ABA inhibition of K_{in}^+ channel currents in the WT as recorded in (A) (open circles, control; filled circles, ABA). (C) K_{in}^+ channel currents in P1#18 treated without (top trace) or with 10 μM ABA (bottom trace). (D) Steady-state current–voltage relationship for ABA inhibition of K_{in}^+ channel currents in P1#18 GCPs as recorded in (C) (open circles, control; filled circles, ABA). (E) K_{in}^+ channel currents in the WT treated without (top trace) or with 10 μM acrolein (bottom trace). (F) Steady-state current–voltage relationship for acrolein inhibition of K_{in}^+ channel currents in the WT as recorded in (E) (open circles, control; filled circles, acrolein). (G) K_{in}^+ channel currents in P1#18 treated without (top trace) or with 10 μM acrolein (bottom trace). (H) Steady-state current–voltage relationship for acrolein inhibition of K_{in}^+ channel currents in P1#18 as recorded in (G) (open circles, control; filled circles, acrolein). The voltage protocol was stepped up from 0 to −180 mV in 20 mV decrements (holding potential, −40 mV). GCPs were treated with ABA and acrolein for 2 h before recordings. Each datum point was obtained from at least four GCPs. Error bars represent the SEM.

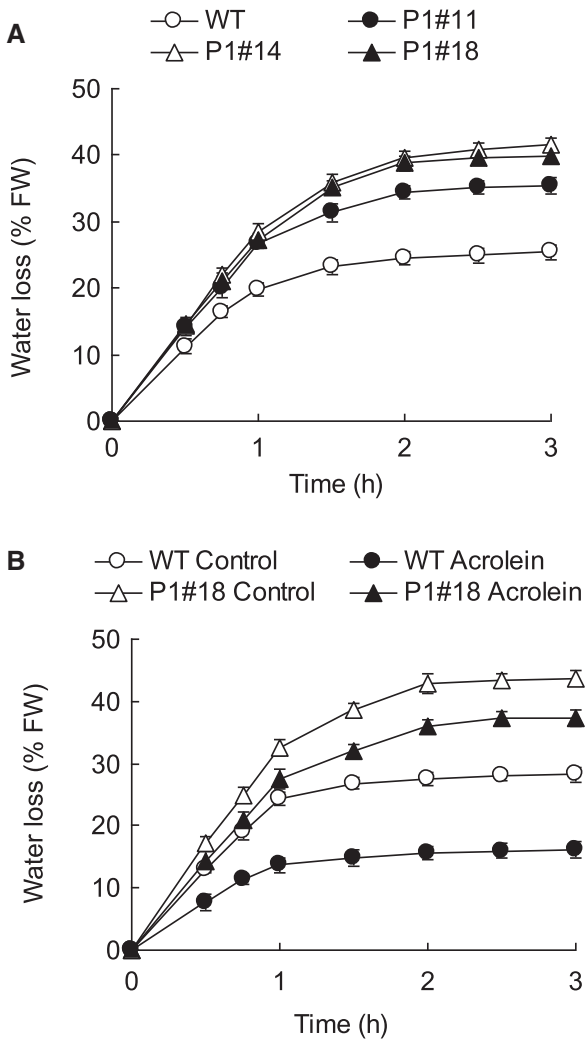

Fig. 9 Overexpression of AER decreases drought tolerance. (A) Water loss from detached leaves of wild-type (WT) and AER-OE plants P1#11, P1#14 and P1#18. (B) Acrolein inhibition of water loss from detached leaves of the WT and P1#18. The masses of detached leaves were recorded over time to calculate the percentage water loss. Averages from three independent experiments are shown. Error bars represent the SEM. FW denotes Fresh weight.

RCS are involved in the downstream ABA signaling event, suppression of K_{in}^+ channels, in guard cells.

We also tested the reversibility of acrolein inhibition of K_{in}^+ channel currents in WT GCPs. Treatment with 10 μM acrolein suppressed K_{in}^+ channel currents in WT GCPs ($P < 0.05$ at −180 mV) (**Supplementary Fig. S5**). Replacement of the bathing solution with acrolein with that without acrolein restored amplitudes of K_{in}^+ channel currents to control levels ($P < 0.05$ at −180 mV) (**Supplementary Fig. S5**). These results also suggest that RCS function physiologically as second messengers in the ABA signaling pathway in guard cells.

Enhancement of transpirational water loss by overexpression of AER

Stomatal closure suppresses transpirational water loss under drought stress. We examined the response of AER-OE plants to drought. Water loss in detached leaves of P1#18 was faster than that in detached leaves of the WT (**Fig. 9A**). These results show that drought stress-induced stomatal closure is mediated by RCS.

We further examined whether acrolein inhibits water loss in detached leaves of the WT and the AER-OE plant, P1#18. Excised leaves of the WT and P1#18 were treated with 100 μM acrolein. Although application of 100 μM acrolein inhibited water loss in WT and P1#18 leaves, water loss in P1#18 was much faster than that in the WT (**Fig. 9B**).

Discussion

Lipid peroxides, the precursors of RCS, are formed via oxidation of membrane lipids in the presence of an increased amount of ROS. In guard cells, ABA activates NAD(P)H oxidases to generate the superoxide radical, which in its protonated form ($HO_2\cdot$) can oxidize lipids. Alternatively, superoxide is converted to H_2O_2 by superoxide dismutase, and forms the hydroxyl radical ($OH\cdot$), the most highly oxidizing ROS, via the metal ion- (such as Fe^{2+}) or peroxidase-catalyzed Fenton reaction. Hence, ABA and ROS can induce RCS generation in guard cells and RCS are likely to function as second messengers in the ABA signaling pathway in guard cells.

On the other hand, lipid peroxides can be formed enzymatically by lipoxygenases (LOXs), resulting in production of RCS. It has been reported that knockout mutations of a *LOX*, *LOX1*, impaired stomatal closure induced by a bacterial elicitor, flg22, but not ABA in Arabidopsis (Montillet et al. 2013). These results suggest that the enzymatic pathway does not contribute to RCS production in guard cell ABA signaling. In the present study, suppression of ROS production impaired RCS production in ABA-treated guard cells (**Fig. 7A**), which suggests that RCS production is mainly mediated by ROS in guard cell ABA signaling.

RCS deplete GSH through conjugation in the tobacco hypersensitive response (Davoine et al. 2006) and ABA-induced stomatal closure is accompanied by depletion of GSH in Arabidopsis guard cells (Akter et al. 2012). Hence, RCS produced in response to ABA may deplete GSH through conjugation in guard cells. Moreover, the amounts of intracellular GSH do not affect ABA-induced ROS production in Arabidopsis guard cells (Akter et al. 2012), which is also in agreement with the ABA signaling model that RCS functions downstream of ROS production.

ABA and H_2O_2 suppress K_{in}^+ channel currents in the guard cell plasma membrane, which is favorable for stomatal closure (Zhang et al. 2001, Saito et al. 2008, Uraji et al. 2012, Yin et al. 2013). ABA induced H_2O_2 production in guard cells of the WT and AER-OE (**Fig. 6A**), while ABA significantly increased the contents of RCS in epidermal tissues of the WT but not in those of AER-OE (**Figs. 3, 4**) and ABA suppressed guard cell K_{in}^+ channel currents in the WT GCPs but not in those of the AER-OE plant P1#18 (**Fig. 8**). Moreover, acrolein also suppressed K_{in}^+ channel currents in WT GCPs but not in P1#18 GCPs (**Fig. 8**). These results suggest that RCS are involved in the downstream

ABA signaling events such as suppression of K_{in}^+ channels. A whole-cell patch-clamp study revealed that K_{in}^+ channel current was inhibited by 100 μM acrolein in Arabidopsis GCPs and a two-electrode voltage clamp study showed that an Arabidopsis K_{in}^+ channel, KAT1, expressed in *Xenopus leavis* oocytes, was also inhibited by 100 μM acrolein (Islam et al. 2015). These results suggest that K_{in}^+ channels are targets of RCS in plants.

This study shows that RCS functions downstream of ROS production in the ABA signaling cascade in guard cells, and previous studies also show that RCS function downstream of ROS in aluminum-induced root injury response in tobacco and salt-induced programmed cell death (Yin et al. 2010, Biswas and Mano 2015). Production of ROS is involved in responses to a variety of abiotic and biotic stimuli in plants (Pei et al. 2000, Ye et al. 2013, Hossain et al. 2014, Khokon et al. 2015). Hence, physiological responses to the stimuli are expected to be accompanied by RCS production.

In conclusion, RCS function as signal mediators downstream of H_2O_2 production in the ABA signaling pathway in guard cells.

Materials and Methods

Plant materials and growth conditions

Three lines of transgenic tobacco (*N. tabacum*) overexpressing Arabidopsis (*A. thaliana*) AER-OE plants (Mano et al. 2005; P1#11, P1#14 and P1#18), and WT tobacco were grown on soil containing 70% (v/v) vermiculite (Asahi-kogyo) and 30% (v/v) Kureha soil (Kureha Chemical) in a growth chamber at 21 ± 2°C and 60% relative humidity with a 16 h light period with 80 μmol m^{-2} s^{-1} photon flux density and 8 h of darkness. Water containing 0.1% Hyponex (Hyponex Japan) was applied to the plant growth tray 2–3 times a week.

Measurement of stomatal aperture

Stomatal apertures were measured as described previously (Uraji et al. 2012). Excised leaves of 5- to 7-week-old plants were floated on an assay solution containing 5 mM KCl, 50 μM $CaCl_2$ and 10 mM MES (pH 6.15 adjusted with Tris). The leaves were incubated in the light for 2 h to open the stomata. Then ABA (Sigma), H_2O_2 or acrolein (Tokyo Chemical Industry) or HNE (Enzo Life Science) was added, and the leaves were kept in the light for 2 h before measurement. The NAD(P)H oxidase inhibitor DPI (Sigma) was added 30 min prior to acrolein application. For measurement of stomatal apertures, the leaves were shredded in a commercial blender for 25 s, and epidermal tissues were collected using nylon mesh.

Measurement of AER activities

Excised leaves of 5- to 7-week-old tobacco were blended for 25 s and epidermal tissues were collected and floated on an assay solution containing 5 mM KCl, 50 μM $CaCl_2$ and 10 mM MES, pH 6.15 (adjusted with Tris), for 2 h in the light followed by the addition of 50 μM ABA or 1 mM H_2O_2 for 2 h. Then, AER activity was measured as described previously (Mano et al. 2005), with some modification. Epidermal tissue was homogenized and extracted in 50 mM potassium phosphate, pH 7.0, containing 10% (w/v) polyvinylpolypyrrolidone. Homogenates were passed through a layer of Miracloth (Calbiochem), and cell debris was pelleted by centrifugation at 8,000×*g* for 10 min. The supernatant was desalted by passing it through a Sephadex G25 column equilibrated with 50 mM potassium phosphate, pH 7.0. AER activity was assayed by the oxidation rate of NADPH at 340 nm in a reaction mixture (1 ml) containing 50 mM MES, pH 6.0 (adjusted with NaOH), 0.1 mM NADPH and 0.1 mM electron acceptor (Mano et al. 2005). Protein was determined using Coomassie Brilliant Blue protein assay solution (Nacalai Tesque) with bovine serum albumin as a standard.

Reactive carbonyl species identification and quantification by HPLC

Excised leaves of 5- to 7-week-old tobacco were blended for 25 s and epidermal tissues were collected and floated on an assay solution containing 5 mM KCl, 50 μM $CaCl_2$ and 10 mM MES, pH 6.15 (adjusted with Tris), for 2 h in the light followed by the addition of 50 μM ABA or 1 mM H_2O_2 for 5, 30, 60 and 120 min. The NAD(P)H oxidase inhibitor DPI (Sigma) was added 30 min prior to ABA application. Then, epidermal tissues were used for RCS analysis. RCS were extracted from the epidermal tissues and derivatized with DNPH, and then identified and quantified by reverse-phase HPLC according to the method of Matsui et al. (2009), with some modifications. Epidermal tissues (0.5 g) were homogenized in acetonitrile (5 ml) containing 2-ethylhexanal (40 nmol; as the internal standard) and 0.005% (w/v) butylhydroxytoluene, and then incubated in a screwcapped glass tube at 60 °C for 30 min. Extract was collected through a glass filter in another glass tube. DNPH (final concentration of 0.5 mM) and formic acid (final concentration 0.5 M) were added, and the solution was mixed well and incubated at 25 °C for 60 min. Then, 5 ml of saturated NaCl solution and 0.8 g of $NaHCO_3$ were added to neutralize the formic acid and incubated at 25 °C for 20 min. After centrifugation, the upper acetonitrile layer was collected and dried in vacuo. The residue was dissolved in 500 μl of acetonitrile and passed through a BondEluteC18 cartridge (sorbent mass 200 mg; Varian), which had been pre-washed with 2 ml of acetonitrile. The material passed through the cartridge was collected, and 10 μl aliquots were injected to HPLC in a Wakosil DNPH-II column (4.6×150 mm; Wako Pure Chemical). Wakosil DNPH-II Eluents A and B (Wako) were used to separate out the compounds, with 100% A (0–5 min), a linear gradient from 100% A to 100% B (5–20 min) and subsequently 100% B (20–35 min) at a flow rate of 1.0 ml min^{-1}. Dinitrophenylhydrazone (DNP) derivatives of RCS were detected at 340 nm. Each RCS corresponding to the peaks is identified based on their retention time, as compared with those of DNP derivatives of authentic carbonyl species. To determine the content of an RCS (nmol g FW^{-1}) from its peak area, the ratio of the peak area to the peak area of the internal standard was first determined. The amount of a RCS was obtained by multiplying this ratio by the added amount of internal standard, i.e. 40 nmol 0.5 g FW^{-1}. For the identified RCS, the amount was further corrected for the DNP derivatization efficiency of the RCS and the extraction efficiency and absorption coefficient of the derivative relative to those of the internal standard (Matsui et al. 2009).

Measurement of viability of guard cells

Viability of guard cells was investigated using FDA (Sigma) as described previously (Hoque et al. 2012) with modifications. Just prior to stomatal aperture measurement after 2 h acrolein and HNE treatment, the epidermal tissues were stained with 10 μM FDA. Guard cells were observed under a fluorescence microscope (Biozero BZ-8000; KEYENCE). Guard cells exhibiting green fluorescence within 5 min were considered as viable.

Measurement of H_2O_2

H_2O_2 production in guard cells was analyzed by using H_2DCF-DA (Sigma) as described previously (Uraji et al. 2012). The epidermal peels were incubated for 3 h in the assay solution containing 5 mM KCl, 50 μM $CaCl_2$ and 10 mM MES (pH 6.15 adjusted with Tris), and then 50 μM H_2DCF-DA was added to the sample. The epidermal tissues were incubated for 30 min at room temperature, and then the excess dye was washed out with the solution. Collected tissues were again incubated with solution and 50 μM ABA for 20 min in the dark condition. The image was captured using a fluorescence microscope (Biozero BZ-8000; KEYENCE), and the pixel intensity of the fluorescence in guard cells was measured using ImageJ 1.42q (National Institutes of Health).

Patch-clamp measurement

Tobacco GCPs were prepared from leaves of 5- to 7-week-old tobacco plants as described previously (Ueno et al. 2005) with some modifications. Fully expanded leaves of tobacco were shredded for 1– 2 min in a blender in 300 ml of cold distilled water. The epidermal tissues were collected on a 100 μm nylon mesh, rinsed with cool distilled water and incubated in first-step digestion medium at 24 °C for 1 h with a shaking speed of 70 strokes min^{-1}. The

epidermal tissues were then collected on 100 μm nylon mesh. To adjust the osmotic pressure, the epidermal tissues were suspended in 0.3 M mannitol containing 1 mM $CaCl_2$ for 30 min on ice. The epidermal tissues on the nylon mesh were collected and incubated in second-step digestion medium at 27 °C for 2–2.5 h with a shaking speed of 50 strokes min^{-1}. When most of the guard cells became rounded, the peels in the second-step digestion solution were gently passed several times through a glass pipette to release GCPs, after which the peels were removed by a 100 μm nylon mesh. The filtrate was further passed through two layers of 30 μm nylon mesh, and the released GCPs were collected by centrifugation for 6 min at 600×*g*. The pellet was washed three times with 0.4 M mannitol containing 1 mM $CaCl_2$. The isolated GCPs were stored in 0.4 M mannitol containing 1 mM $CaCl_2$ on ice in the dark until use. Whole-cell currents were recorded using a CEZ-2200 or CEZ-2400 patch-clamp amplifier (Nihon Kohden). No leak subtraction was applied for all current–voltage curves. For data analysis, pCLAMP 8.2 or pCLAMP 10.3 software (Molecular Devices) was used. Pipette solution contained 30 mM KCl, 70 mM monopotassium glutamate, 2 mM $MgCl_2$, 3.35 mM $CaCl_2$, 6.7 mM ethylene glycol EGTA and 10 mMHEPES (pH 7.1 adjusted with Tris). Bath solution contained 30 mM KCl, 2 mM $MgCl_2$, 40 mM $CaCl_2$ and 10 mM MES (pH 5.5 adjusted with Tris). Osmolarity was adjusted to 500 mmol kg^{-1} (pipette solutions) and 485 mmol kg^{-1} (bath solutions) with D-sorbitol.

Water loss measurement

For measurements of water loss from detached leaves of wild-type and AER-OE plants P1#11, P1#14 and P1#18, excised leaves of 5- to 7-week-old plants were placed on a bench with the abaxial side facing up, and their masses were recorded over time to calculate the percentage water loss. For acrolein treatment, excised leaves of 5- to 7-week-old WT and P1#18 were floated on an assay solution containing 5 mM KCl, 50 μM $CaCl_2$ and 10 mM MES (pH 6.15 adjusted with Tris) in the light for 2 h. Then acrolein (Tokyo Chemical Industry) was added, and the leaves were kept in the light for 2 h before taking their masses over time. Water losses were expressed as a percentage of initial fresh weight.

Statistical analysis

The significance of differences between mean values was assessed by Student's *t*-test analysis in all parts of this article. We regarded differences at the level of $P < 0.05$ as significant.

Supplementary data

Supplementary data are available at PCP online.

Funding

This work was supported by the Japan Society for the Promotion of Science [Grants-in-Aid for Fellows (to W.Y.) and by Grants-in Aid for Scientific Research (C) No. 26440149 (to J.M.)].

Disclosures

The authors have no conflicts of interest to declare.

References

Akter, N., Sobahan, M.A., Uraji, M., Ye, W., Hossain, M.A., Mori, I.C., et al. (2012) Effects of depletion of glutathione on abscisic acid- and methyl jasmonate-induced stomatal closure in Arabidopsis thaliana. *Biosci. Biotechnol. Biochem.* 76: 2032–2037.

Assmann, S.M. and Shimazaki, K. (1999) The multisensory guard cell. Stomatal responses to blue light and abscisic acid. *Plant Physiol.* 119: 809–815.

Biswas, M.S. and Mano, J. (2015) Lipid peroxide-derived short-chain carbonyls mediate H2O2-induced and NaCl-induced programmed cell death in plants. *Plant Physiol.* 168: 885–898.

Biswas, M.S. and Mano, J. (2016) Reactive carbonyl species activate caspase-3-like protease to initiate programmed cell death in plants. *Plant Cell Physiol.* 57: 1432–1442.

Cutler, S.R., Rodriguez, P.L., Finkelstein, R.R. and Abrams, S.R. (2010) Abscisic acid: emergence of a core signaling network. *Annu. Rev. Plant. Biol.* 61: 651–679.

Davoine, C., Falletti, O., Douki, T., Iacazio, G., Ennar, N., Montillet, J.L., et al. (2006) Adducts of oxylipin electrophiles to glutathione reflect a 13 specificity of the downstream lipoxygenase pathway in the tobacco hypersensitive response. *Plant Physiol.* 140: 1484–1493.

Hoque, T.S., Uraji, M., Ye, W., Hossain, M.A., Nakamura, Y. and Murata, Y. (2012) Methylglyoxal-induced stomatal closure accompanied by peroxidase-mediated ROS production in Arabidopsis. *J. Plant Physiol.* 169: 979–986.

Hossain, M.A., Ye, W., Munemasa, S., Nakamura, Y., Mori, I.C. and Murata, Y. (2014) Cyclic adenosine 5′-diphosphoribose (cADPR) cyclic guanosine 3′,5′-monophosphate positively function in Ca^{2+} elevation in methyl jasmonate-induced stomatal closure, cADPR is required for methyl jasmonate-induced ROS accumulation NO production in guard cells. *Plant Biol. (Stuttg.)* 16: 1140–1144.

Huang, W., Ma, X., Wang, Q., Gao, Y., Xue, Y., Niu, X., et al. (2008) Significant improvement of stress tolerance in tobacco plants by overexpressing a stress-responsive aldehyde dehydrogenase gene from maize (Zea mays). *Plant Mol. Biol.* 68: 451–463.

Hubbard, K.E., Nishimura, N., Hitomi, K., Getzoff, E.D. and Schroeder, J.I. (2010) Early abscisic acid signal transduction mechanisms: newly discovered components and newly emerging questions. *Genes Dev.* 24: 1695–1708.

Islam, M.M., Ye, W., Matsushima, D., Khokon, M.A., Munemasa, S., Nakamura, Y., et al. (2015) Inhibition by acrolein of light-induced stomatal opening through inhibition of inward-rectifying potassium channels in Arabidopsis thaliana. *Biosci. Biotechnol. Biochem.* 79: 59–62.

Khokon, M.A.R., Salam, M.A., Jammes, F., Ye, W., Hossain, M.A., Uraji, M., et al. (2015) Two guard cell mitogen-activated protein kinases, MPK9 and MPK12, function in methyl jasmonate-induced stomatal closure in Arabidopsis thaliana. *Plant Biol. (Stuttg.)* 17: 946–952.

Kwak, J.M., Mori, I.C., Pei, Z.M., Leonhardt, N., Torres, M.A., Dangl, J.L., et al. (2003) NADPH oxidase AtrbohD and AtrbohF genes function in ROS-dependent ABA signaling in Arabidopsis. *EMBO J.* 22: 2623–2633.

Mano, J. (2012) Reactive carbonyl species: their production from lipid peroxides, action in environmental stress, and the detoxification mechanism. *Plant Physiol. Biochem.* 59: 90–97.

Mano, J., Belles-Boix, E., Babiychuk, E., Inze, D., Torii, Y., Hiraoka, E., et al. (2005) Protection against photooxidative injury of tobacco leaves by 2-alkenal reductase. Detoxication of lipid peroxide-derived reactive carbonyls. *Plant Physiol.* 139: 1773–1783.

Mano, J., Torii, Y., Hayashi, S., Takimoto, K., Matsui, K., Nakamura, K., et al. (2002) The NADPH:quinone oxidoreductase P1-zeta-crystallin in Arabidopsis catalyzes the alpha,beta-hydrogenation of 2-alkenals: detoxication of the lipid peroxide-derived reactive aldehydes. *Plant Cell Physiol.* 43: 1445–1455.

Matsui, K., Sugimoto, K., Kakumyan, P., Khorobrykh, S.A. and Mano, J. (2009) Volatile oxylipins and related compounds formed under stress in plants. *Methods Mol. Biol.* 580: 17–28.

Melotto, M., Underwood, W. and He, S.Y. (2008) Role of stomata in plant innate immunity and foliar bacterial diseases. *Annu. Rev. Phytopathol.* 46: 101–122.

Montillet, J.L., Leonhardt, N., Mondy, S., Tranchimand, S., Rumeau, D., Boudsocq, M., et al. (2013) An abscisic acid-independent oxylipin pathway controls stomatal closure and immune defense in Arabidopsis. *PLoS Biol.* 11: e1001513.

Mosblech, A., Feussner, I. and Heilmann, I. (2009) Oxylipins: structurally diverse metabolites from fatty acid oxidation. *Plant Physiol. Biochem.* 47: 511–517.

Mueller, M.J. (2004) Archetype signals in plants: the phytoprostanes. *Curr. Opin. Plant Biol.* 7: 441–448.

Murata, Y., Mori, I.C. and Munemasa, S. (2015) Diverse stomatal signaling and the signal integration mechanism. *Annu. Rev. Plant Biol.* 66: 369–392.

Murata, Y., Pei, Z.M., Mori, I.C. and Schroeder, J.I. (2001) Abscisic acid activation of plasma membrane Ca^{2+} channels in guard cells requires cytosolic NAD(P)H and is differentially disrupted upstream and downstream of reactive oxygen species production in *abi1-1* and *abi2-1* protein phosphatase 2C mutants. *Plant Cell* 13: 2513–2523.

Nambara, E. and Marion-Poll, A. (2005) Abscisic acid biosynthesis and catabolism. *Annu. Rev. Plant Biol.* 56: 165–185.

Oberschall, A., Deak, M., Torok, K., Sass, L., Vass, I., Kovacs, I., et al. (2000) A novel aldose/aldehyde reductase protects transgenic plants against lipid peroxidation under chemical and drought stresses. *Plant J.* 24: 437–446.

Papdi, C., Ábrahám, E., Joseph, M.P., Popescu, C., Koncz, C. and Szabados, L., et al. (2008) Functional identification of Arabidopsis stress regulatory genes using the controlled cDNA overexpression system. *Plant Physiol.* 147: 528–542.

Pei, Z.M., Murata, Y., Benning, G., Thomine, S., Klüsener, B., Allen, G.J., et al. (2000) Calcium channels activated by hydrogen peroxide mediate abscisic acid signalling in guard cells. *Nature* 406: 731–734.

Saito, N., Munemasa, S., Nakamura, Y., Shimoishi, Y., Mori, I.C. and Murata, Y. (2008) Roles of RCN1, regulatory A subunit of protein phosphatase 2A, in methyl jasmonate signaling and signal crosstalk between methyl jasmonate and abscisic acid. *Plant Cell Physiol.* 49: 1396–1401.

Schroeder, J.I., Kwak, J.M. and Allen, G.J. (2001) Guard cell abscisic acid signalling and engineering drought hardiness in plants. *Nature* 410: 327–330.

Shimazaki, K., Doi, M., Assmann, S.M. and Kinoshita, T. (2007) Light regulation of stomatal movement. *Annu. Rev. Plant. Biol.* 58: 219–247.

Stiti, N., Adewale, I.O., Petersen, J., Bartels, D. and Kirch, H.H. (2011) Engineering the nucleotide coenzyme specificity and sulfhydryl redox sensitivity of two stress-responsive aldehyde dehydrogenase isoenzymes of Arabidopsis thaliana. *Biochem. J.* 434: 459–471.

Turóczy, Z., Kis, P., Török, K., Cserháti, M., Lendvai, Á., Dudits, D., et al. (2011) Overproduction of a rice aldo–keto reductase increases oxidative and heat stress tolerance by malondialdehyde and methylglyoxal detoxification. *Plant Mol. Biol.* 75: 399–412.

Ueno, K., Kinoshita, T., Inoue, S., Emi, T. and Shimazaki, K. (2005) Biochemical characterization of plasma membrane H^+-ATPase activation in guard cell protoplasts of *Arabidopsis thaliana* in response to blue light. *Plant Cell Physiol.* 46: 955–963.

Uraji, M., Katagiri, T., Okuma, E., Ye, W., Hossain, M.A., Masuda, C., et al. (2012) Cooperative function of PLDδ and PLDα1 in abscisic acid-induced stomatal closure in Arabidopsis. *Plant Physiol.* 159: 450–460.

Yadav, U.C. and Ramana, K.V. (2013) Regulation of NF-kappaB-induced inflammatory signaling by lipid peroxidation-derived aldehydes. *Oxid. Med. Cell Longev.* 2013: 690545.

Yamauchi, Y., Hasegawa, A., Taninaka, A., Mizutani, M. and Sugimoto, Y. (2011) NADPH-dependent reductases involved in the detoxification of reactive carbonyls in plants. *J. Biol. Chem.* 286: 6999–7009.

Ye, W., Adachi, Y., Munemasa, S., Nakamura, Y., Mori, I.C. and Murata, Y. (2015) Open Stomata 1 Kinase is essential for yeast elicitor-induced stomatal closure in Arabidopsis. *Plant Cell Physiol.* 56: 1239–1248.

Ye, W., Muroyama, D., Munemasa, S., Nakamura, Y., Mori, I.C. and Murata, Y. (2013) Calcium-dependent protein kinase, CPK6, positively functions in induction by YEL of stomatal closure and inhibition by YEL of light-induced stomatal opening in Arabidopsis. *Plant Physiol.* 163: 591–599.

Yin, L., Mano, J., Wang, S., Tsuji, W. and Tanaka, K. (2010) The involvement of lipid peroxide-derived aldehydes in aluminum toxicity of tobacco roots. *Plant Physiol.* 152: 1406–1417.

Yin, Y., Adachi, Y., Ye, W., Hayashi, M., Nakamura, Y., Kinoshita, T., et al. (2013) Difference in abscisic acid perception mechanisms between closure induction and opening inhibition of stomata. *Plant Physiol.* 163: 600–610.

Zhang, X., Miao, Y.C., An, G.Y., Zhou, Y., Shangguan, Z.P., Gao, J.F., et al. (2001) K^+ channels inhibited by hydrogen peroxide mediate abscisic acid signaling in Vicia guard cells. *Cell Res.* 11: 195–202.